ngVLA Antenna Memo #17 (Version 1)
ngVLA Pointing System Recommendation

Jeff Mangum (NRAO)

January 16, 2025

Abstract

This document provides a recommendation for the structure and implementation of the antenna pointing module for the ngVLA Online Data Acquisition System. See change record after acknowledgments for changes incorporated in this version of the memo.

1 Summary

A recommendation for the ngVLA monitor and control system calculations which properly position the ngVLA antennas to point to a particular place on the sky is provided. This recommendation includes a description of the ngVLA prototype antenna contractor-supplied metrology systems and how those systems are integrated into the ngVLA pointing system. This document also describes a number of ancillary antenna pointing issues, including pointing offsets necessary to correct for frontend positioning, corrections due to the local gravitational deflection of the vertical at each antenna, a demonstration of the pitfalls encountered when using the small angle approximation in an antenna pointing model, and on-axis tiltmeter calibration procedures. The recommended pointing system described is an adaptation of that implemented on the Atacama Large Millimeter/submillimeter Array (ALMA).

2 Design Considerations

The pointing system design described in this document is meant to provide an efficient system for deriving and tracking antenna pointing performance both during antenna acceptance testing,

commissioning, and operations. The philosophy embedded in this pointing system design is based on the following principles:

- **It is time to abandon the small-angle approximation used in antenna pointing models:** Many telescopes, including the VLA, ALMA, and NRAO 12m, use the small-angle approximations to what is a rotation matrix from the input [HA,Dec] coordinates to the [Az,El] position demanded by the antenna. This small-angle approximation has limitations which grow more significant at high elevation (see Section C).
- **Metrology is the antenna contractor's responsibility:** Since any metrology system was included in an antenna design by the antenna contractor, it is best to let that contractor apply any metrology corrections. Normally those corrections are made directly to the antenna's (Az,El) positions within the contractor's antenna computer (ACU, or Antenna Control Unit).
- **Refraction corrections are the user's responsibility:** Since the users of an antenna system have the requisite experience to derive and apply refraction corrections to the antenna (Az,El) positions, the user should be responsible for this task.
- **The antenna pointing models need to be implemented and maintained by the user:** As antenna pointing models can be dynamic (especially when commissioning a new antenna), the antenna pointing model is best implemented and maintained by the user. Additionally, pointing models correct for predictable, slowly-varying antenna deformations. Any antenna deformations that vary on shorter time scales, such as those corrected through metrology, are best corrected within the ACU.
- **Absolute pointing models allow for antenna performance assessment and tracking:** To allow for tracking antenna performance and stability over time (i.e., changing environmental conditions, during operations, etc.), pointing models need to be functions of absolute rather than relative pointing coefficients. Changes in pointing model coefficients are often the first, or even only, indication of the degradation in an antenna system.
- **Astronomical calculations are the user's responsibility:** The intricacies of converting (RA,Dec) to (Az,El) require an astronomer's skill set.

3 A Rigorous Pointing Model Solution

The traditional antenna pointing model development (Stumpff, 1972) assumed that the small-angle approximation applied. This allowed for the pointing equations to be written as two linear equations which could be solved with a simple matrix inversion. In the 52 years since this original formalism was developed and widely adopted, computing has improved. It is now possible to solve the transformation from the input [RA,Dec] coordinates to the [Az,El] position demanded by the antenna exactly, as described in Wallace (2002) using the Simple Pointing Kernel (SPK), an application of the Standards of Fundamental Astronomy (SOFA: http://www.tpointsw.uk/sofa.htm) package. Much of this document uses the small-angle approximation in its examples, **but the recommendation is to use the rigorous algorithm for the ngVLA pointing model solution.**

4 Azimuth Coordinate Definition

There are multiple possible definitions for the azimuth coordinate system on a telescope. One azimuth coordinate definition defines azimuth increasing as the antenna rotates clockwise when viewed from above. Differences arise when defining the zero-point for the azimuth coordinate. ALMA and the NRAO 12 m define $Az = 0$ toward the north, which places $Az = 90$ toward the east (Pangole, 2003). The ngVLA and VLA, on the other hand, define $Az = 0$ toward the south (Selina & Sturgis, 2020), which places $Az = 90$ toward the west. It is important to understand these differences when deriving the pointing model formalism for a telescope.

5 Pointing System Definitions

A detailed description of a pointing model similar to that used in the following is given in Mangum (2001), which is the antenna pointing system implemented for ALMA. The `TPOINT` pointing analysis system developed by Pat Wallace possesses all of the capabilities necessary to analyze telescope pointing characteristics and has been used at a wide range of observatories for many decades (including ALMA). For the following analysis, we use the `TPOINT` naming and coordinate conventions.

In the following we define how the pointing model, metrology corrections, and the azimuth and elevation positions provided to the telescope encoders are related. Note that the ngVLA azimuth coordinate is defined as $Az = 0$ when pointing south and $Az = 90$ when pointing west (Selina & Sturgis, 2020). The azimuth and elevation which centres the source on the boresight of the antenna is given by

$$A_{com} = A_{demand} + \Delta A + \Delta A_{metrology} \quad (1)$$

$$E_{com} = E_{demand} + \Delta E + \Delta E_{metrology} \quad (2)$$

where

A_{demand} and E_{demand}: Azimuth and elevation demanded encoder position (often referred to as just "encoder" positions). These are the azimuth and elevation positions provided to the antenna encoders which will center a source on the boresight.

A_{com} and E_{com}: Azimuth and elevation position commanded by the customer's computer. Sometimes also referred to as "true", "observed", or "predicted" azimuth and elevation.

ΔA and ΔE: Azimuth and elevation pointing model corrections.

$\Delta A_{metrology}$ and $\Delta E_{metrology}$: Azimuth and elevation corrections applied by the metrology system (usually applied by the contractor ACU).

The pointing correction terms using just the seven 'geometric" pointing terms are defined (to

first order) as follows:

$$\begin{aligned}\Delta A &= -\mathrm{IA} - \mathrm{CA}\sec(E_{com}) - \mathrm{NPAE}\tan(E_{com}) + \mathrm{AN}\tan(E_{com})\sin(A_{com}) \\ &\quad +\mathrm{AW}\tan(E_{com})\cos(A_{com}) + \Delta A_{obs}\sec(E_{com}) + \text{additional terms} \qquad (3)\\ \Delta E &= \mathrm{IE} + \mathrm{AN}\cos(A_{com}) - \mathrm{AW}\sin(A_{com}) + \mathrm{HECE}\cos(E_{com}) \\ &\quad +\mathrm{HESE}\sin(E_{com}) + \Delta E_{obs} + R(P_s, T_s, RH, E_{com}) + \text{additional terms} \qquad (4)\end{aligned}$$

As the need arises, the number of terms necessary to specify the A and E positioning of the antenna can be expanded. The basic and additional (sometimes called "core") pointing coefficients and their values derived from the ALMA production antennas are listed in Tables 1 and 2.

Table 1: The Seven Basic Pointing Model Terms

Term	Correction Formula		Nominal Cause
	ΔAz	ΔEl	
IA	$-\mathrm{IA}$	...	Az encoder zero point offset
IE	...	$+\mathrm{IE}$	El encoder zero point offset
CA	$-\mathrm{CA}\sec E$	...	Non-perpendicularity between the boresight and El axis
NPAE	$-\mathrm{NPAE}\tan E$	...	Non-perpendicularity between the Az and El axes
AN	$+\mathrm{AN}\tan E\sin A$	$+\mathrm{AN}\cos A$	Az axis offset/misalignment north-south (north = positive)
AW	$+\mathrm{AW}\tan E\cos A$	$-\mathrm{AW}\sin A$	Az axis offset/misalignment east-west (west = positive)
HECE	...	$+\mathrm{HECE}\cos E$	Hooke's Law vertical flexure

Pointing terms are derived from a collection of pointing measurements. The ordering of the terms in the `TPOINT` file is as follows: (A_{com}, E_{com}, A_{demand}, E_{demand}; see Appendix A). Pointing measurements used to derive a pointing model must be representative of the telescope pointing behavior over all azimuth and elevation to allow the model fitting software (`TPOINT`) to perform what amounts to a linear least-squares fit to Equations 3 and 4. The terms A_{obs} and E_{obs} are observer-applied corrections based on individual pointing measurements made during an astronomical observing program. The refraction correction term in Equation 4 is usually applied on-line for each position command to the telescope. Several approaches to the derivation of this correction have been made and used at existing radio telescopes, some of which are described in Mangum (2001). The complete analysis of the ALMA prototype antenna pointing performance can be found in Mangum et al. (2006).

6 Positioning Calculation Sequence

The ALMA positioning calculation system is illustrated in Figure 1. The quantities logged for input to `TPOINT` are (i) the observed (Az,El) and (ii) the commanded inputs to the manufacturer's metrology systems, the latter constituting a "smart encoders" interface. For ALMA these "smart encoder" (Az,El) values are derived from the *AZ_POSN_RSP* and *EL_POSN_RSP* ACU monitor points, as they include any improvement produced by the antenna metrology systems. For

Table 2: ALMA Core Pointing Model Terms[a]

Term	Ampl. (arcsec)	Correction Formula[B]	Nominal Cause
HESE	-26.95	$\Delta E = +\mathrm{HESE}\sin E$	El encoder run-out, sine component
HECE	-22.89	$\Delta E = +\mathrm{HECE}\cos E$	El encoder run-out, cosine component and/or vertical flexure
HASA	-2.89	$\Delta A = -\mathrm{HASA}\sin A$	Az encoder run-out, sine component
HACA	-4.18	$\Delta A = +\mathrm{HACA}\cos A$	Az encoder run-out, cosine component
HASA2	$+1.41$	$\Delta A = +\mathrm{HASA2}\sin 2A$	Az encoder tilt, sine component
HACA2	$+1.15$	$\Delta A = -\mathrm{HACA2}\cos 2A$	Az encoder tilt, cosine component
HESA2	$+0.69$	$\Delta E = -\mathrm{HESA2}\sin 2A$	El nod twice per Az rev, sine component
HECA2	$+0.73$	$\Delta E = +\mathrm{HECA2}\cos 2A$	El nod twice per Az rev, cosine component
HASA3	$+0.42$	$\Delta A = -\mathrm{HASA3}\sin 3A$	Az encoder error 3× per rev, sine component
HACA3	$+0.41$	$\Delta A = +\mathrm{HACA3}\cos 3A$	Az encoder error 3× per rev, cosine component
HESA3	-1.41	$\Delta E = +\mathrm{HESA3}\sin 3A$	El nod 3× per Az rev, sine component
HECA3	$+0.25$	$\Delta E = -\mathrm{HECA3}\cos 3A$	El nod 3× per Az rev, cosine component

[a] The core pointing model terms for ALMA listed here were derived from optical pointing telescope measurements.

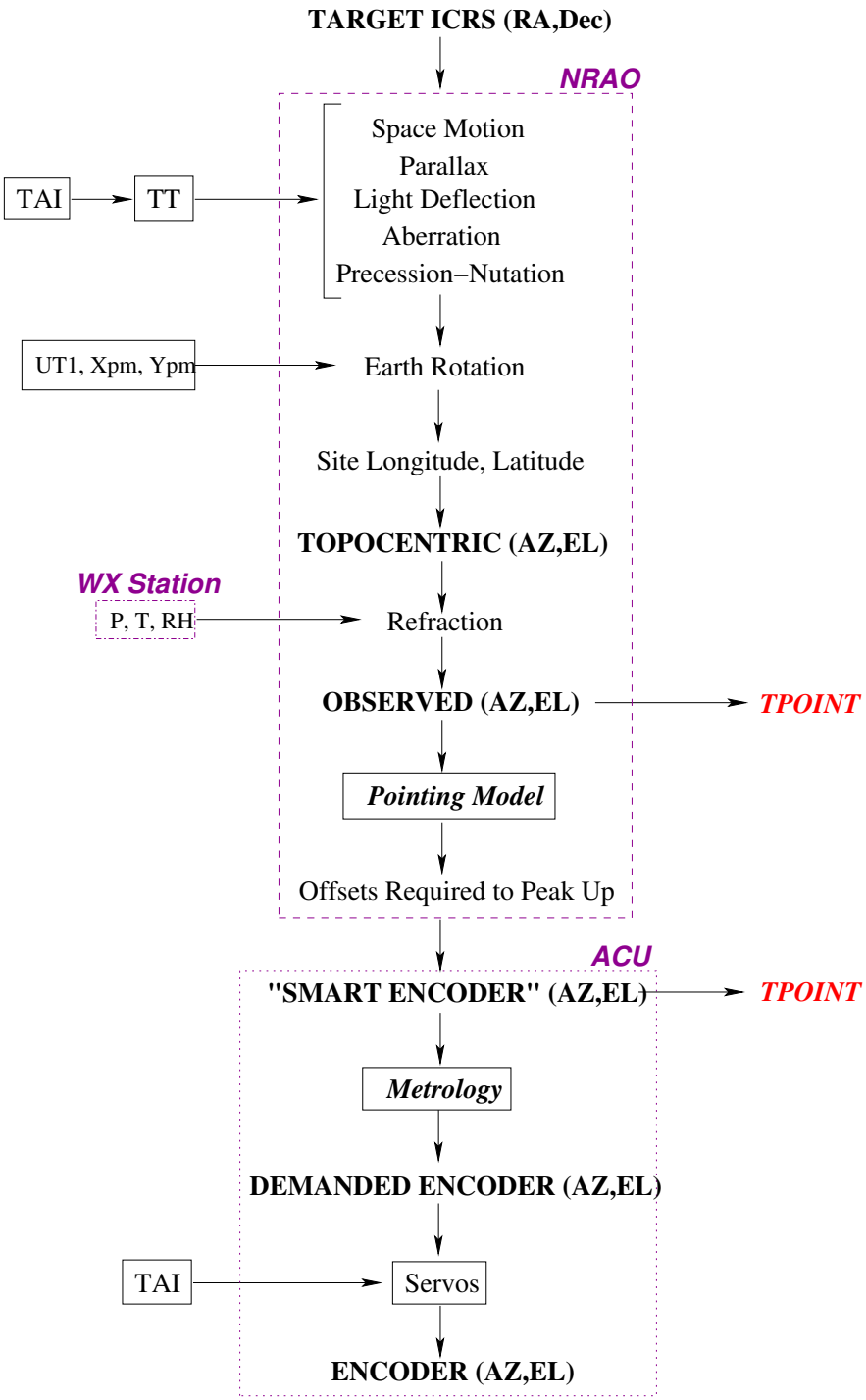

Figure 1: Proposed positioning calculation flow for the ngVLA (adopted from the ALMA antenna positioning system). The roles of the respective computers are shown boxed.

ngVLA the *Correction Manager* (Rogulenko, 2024, Section 3.2.4) handles the application and reporting of metrology corrections and resultant (Az,El) positions.

7 Metrology Sensors

Note: The details of the design and implementation of the ngVLA prototype antenna metrology system are not yet available. This section provides only a summary description of these systems.

In the following we summarize the design of the ngVLA prototype antenna metrology systems. These metrology systems include:

Tiltmeter : A two-axis floor mounted tiltmeter will be installed in the turnhead above the azimuth bearing/cable wrap, centered on the azimuth axis (Section 7.1).

Temperature Sensors : A temperature sensor system will be installed on the antenna mount pedestal (Section 7.2).

The metrology-based pointing offsets ($\Delta A_{metrology}$,$\Delta E_{metrology}$) are given by:

$$\Delta A_{metrology} = \Delta A_{Tiltm} - \Delta A^{*}_{tiltm,rep} + \Delta A_{temp} \quad (5)$$
$$\Delta E_{metrology} = \Delta E_{Tiltm} - \Delta E^{*}_{tiltm,rep} + \Delta E_{temp} \quad (6)$$

In the following we derive each of the terms on the right-hand sides of Equations 6.

7.1 Tiltmeter

There will be one two-axis tiltmeter installed on the ngVLA prototype antenna, positioned above the azimuth bearing on the azimuth axis, as shown in Figure 2. The tiltmeter measurements provide information about the varying tilt of the azimuth axis of the antenna. In addition to the zeroth-order tilt due to misalignment of azimuth axis and/or foundation during installation, there are varying tilts due to temperature and gravitational deformations of the cone structure (i.e. gravitational deflection of the vertical; see Appendix B), bearing runout, etc.. The non-orthogonality due to misalignment is normally part of the pointing error model (Section 5). In order to limit the tiltmeter correction to a mere compensation of non-repeatable effects, the repeatable portion related to the non-orthogonality of the azimuth axis is removed from the total tiltmeter correction. The azimuth and elevation pointing correction measured by the tiltmeter is given by:

$$\Delta A_{Tiltm} = \tan(E_{com}) T1_y \quad (7)$$
$$\Delta E_{Tiltm} = T1_x \quad (8)$$

Tiltmeters are notorious for being highly sensitive to acceleration and changes in temperature. Therefore, they are normally not installed at antenna locations that experience acceleration, and they are often equipped with a temperature sensor, which is used to calibrate the tilts that it measures. Based on information provided in the mtex interface control document which describes

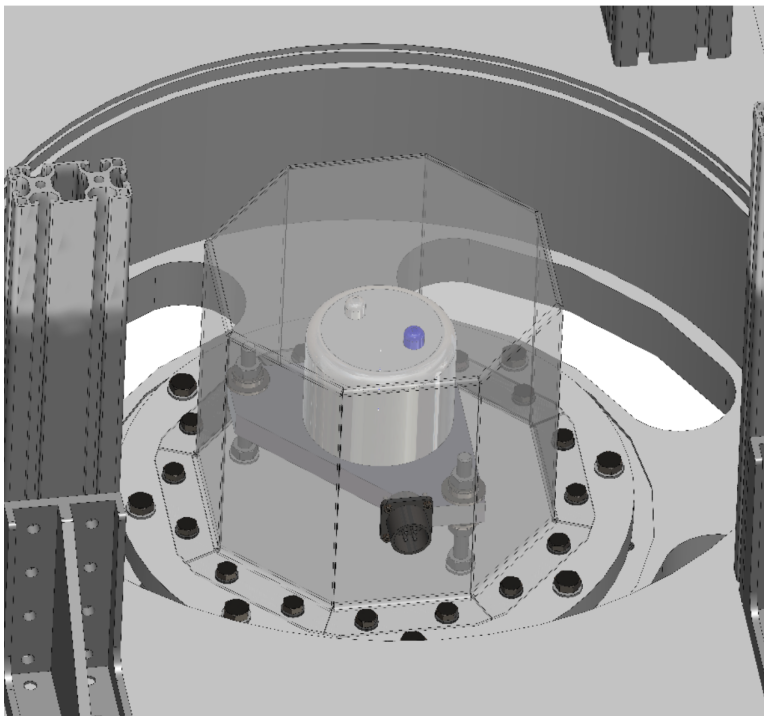

Figure 2: Tiltmeter located in the ngVLA prototype antenna turnhead, above the azimuth encoder/cable wrap.

the antenna monitor and control interface (Rogulenko, 2024), the ngVLA prototype antenna tiltmeter will be a standard Jewell Instruments two-axis tiltmeter. The (x,y,temp) readout from the tiltmeter will be read through the ngVLA antenna control bus by the antenna control unit. The components of the monitor and control system that comprise the temperature sensor-based calibration and measurement of the analog position readout of the tiltmeter are defined in Table 3. The relationship between measured and temperature-calibrated x/y tilt based on the components listed in Table 3 is given by:

$$\text{temp\_corrected\_(x/y)\_tilt} = \text{gain} \times \text{tiltmeter\_(x/y)\_voltage} \times (2 + K_s) - K_z \tag{9}$$

...where...

$$K_s = \text{ks\_(x/y)} \times (\text{tiltmeter\_temperature} - \text{t\_cal}) \tag{10}$$

$$K_z = \text{kz\_(x/y)} \times (\text{tiltmeter\_temperature} - \text{t\_cal}) \tag{11}$$

The tiltmeters measure the *total* tilt of the azimuth axis. This includes deformations due to temperature, wind, and the tilt due to non-orthogonality of the azimuth axis. Since the non-orthogonality of the azimuth axis is part of the customer's pointing model (via the terms AN and AW; see Section 5), a correction must be made by the ACU to remove the nominal azimuth axis tilt. The resultant tilt measurement will then encompass only non-repeatable changes in azimuth axis tilt due to temperature or wind deformation. The repeatable portion of the azimuth axis tilt removed by the ACU is given by:

$$\Delta A^*_{tiltm,rep} = +\text{AN}_0 \tan(E) \sin(A) + \text{AW}_0 \tan(E) \cos(A) \tag{12}$$

$$\Delta E^*_{tiltm,rep} = +\text{AN}_0 \cos(A) - \text{AW}_0 \sin(A) \tag{13}$$

Table 3: ngVLA Prototype Antenna Tiltmeter Metrology Monitor and Control Components[a]

Component	Units	Description
tiltmeter_(x/y)_voltage	V	Measured (x/y)-axis tiltmeter voltage. Low-Gain setting: 1 μrad/mV, High-Gain setting: 0.1 μrad/mV.
tiltmeter_(x/y)_mdeg	mdeg	Measured (x/y)-axis tiltmeter voltage with gain (μrad/mV) applied.
tiltmeter_temperature	C	Built-in temperature sensor measurement.
t_cal	C	In-plant calibration constant for built-in temperature sensor.
ks_(x/y)	C^{-1}	Tiltmeter temperature compensation function slope.
kz_(x/y)	mdeg/C	Tiltmeter temperature compensation function offset.
temp_corrected_(x/y)_tilt	mdeg	Temperature-corrected x/y axis tilt.

[a] From Rogulenko (2024), Table 269, Section 3.7.1.2, page 144.

To derive the values for the tiltmeter calibration constants AN_0, AW_0, dx, and dy one of two techniques can be used. See Appendix D for details. Analyses of the performance of the equivalent tiltmeter systems on the ALMA Vertex prototype antenna are described in Emerson (2004a), Emerson (2004b), Mangum (2003), Greve & Mangum (2004), and Wallace et al. (2004).

7.2 Temperature Sensors

A temperature sensor system will be installed on the ngVLA prototype antenna to correct for temperature-induced deformations of the antenna pedestal (Figure 3). The contractor may install additional temperature sensors to support this metrology system, but those design details are not yet available. An example of the implementation of a temperature sensor metrology system, for the Green Bank Telescope (GBT), is given by White et al. (2022).

8 Receiver Band Layout

The ngVLA production receiver band layout is described in Sturgis (2025b) and shown in Figure 4. The physical offsets for each receiver band are listed in Table 4 (from Sturgis, 2025b). For a fixed frontend the associated (A,E) offsets for each band are then given by (to first order) $\Delta A_{band} = \tan^{-1}(R_{band}/f)$, $\Delta E_{band} = 0$, where f is the focal length of the receiver (in mm). Since the frontend assembly will be repositioned along the Y and Z axes to enable measurements with each receiver band, these band-dependent offsets to the pointing for each band should not be needed.

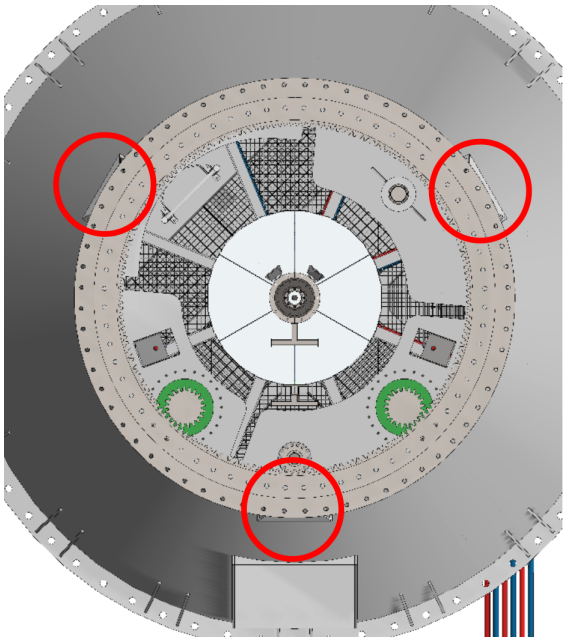

Figure 3: Locations for the three ambient-air temperature sensors (red circles) comprising the temperature sensor metrology system for the ngVLA prototype antenna.

Table 4: ngVLA Prototype and Production Receiver Band Offsets

Band	Frequency Range (GHz)	Window Location (R_{band})[a] (mm)
Prototype Frontend[b]		
X-Band	8–12	+612.083
Q-Band	40–50	+7.401
Production Frontend[c]		
1	1.2–3.5	+605.8
2	3.4–12.3	−671.0
3	12.3–20.5	−442.4
4	20.5–34.0	−213.8
5	30.5–50.5	−1.7
6	70–116	+193.9

[a] Relative to FE focal axis.
[b] From Sturgis (2025a).
[c] From Grammer & Sturgis (2022) and Sturgis (2025b).

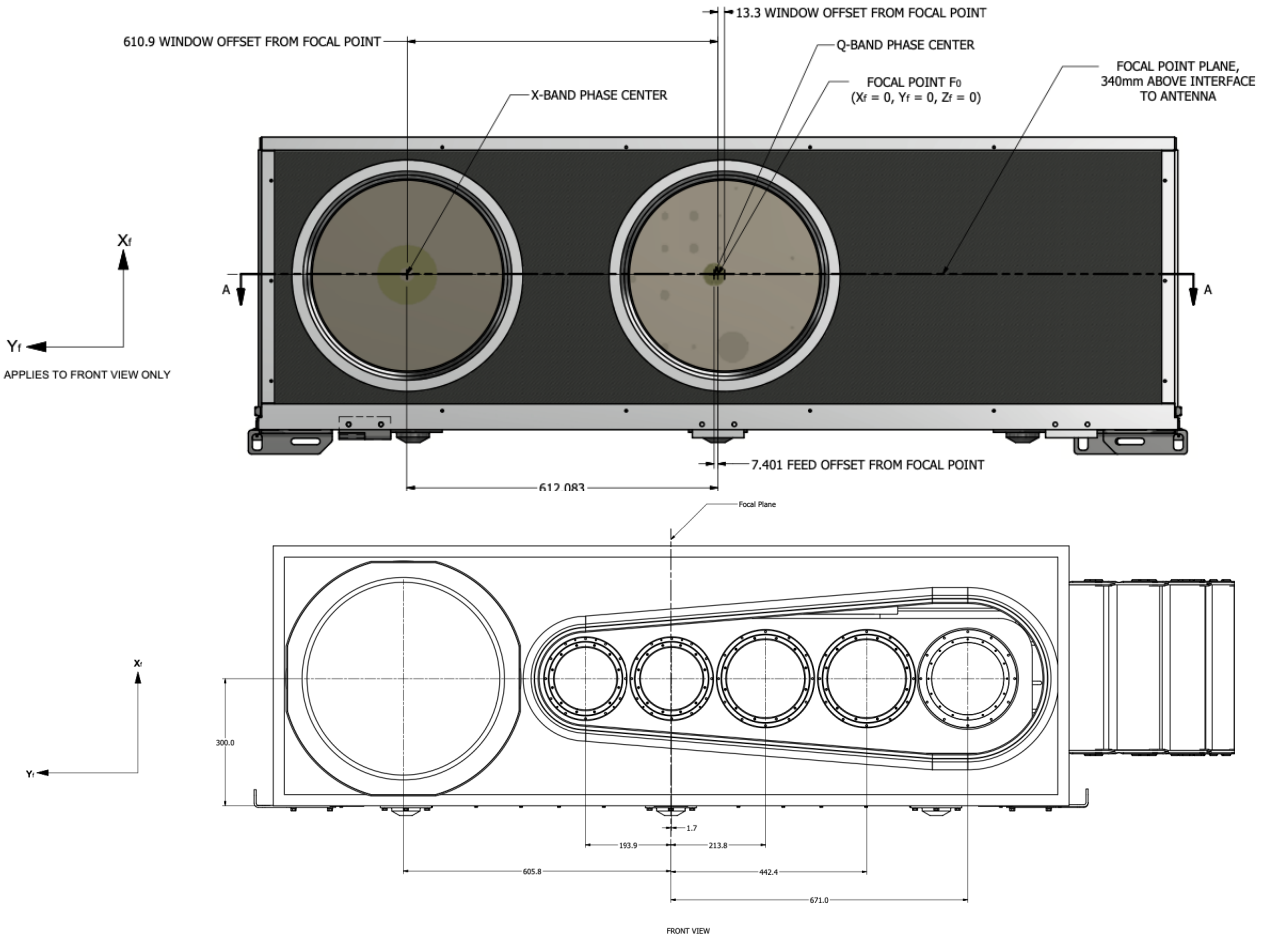

Figure 4: ngVLA prototype (top; Sturgis, 2025a) and production (bottom; Sturgis, 2025b) receiver band layout.

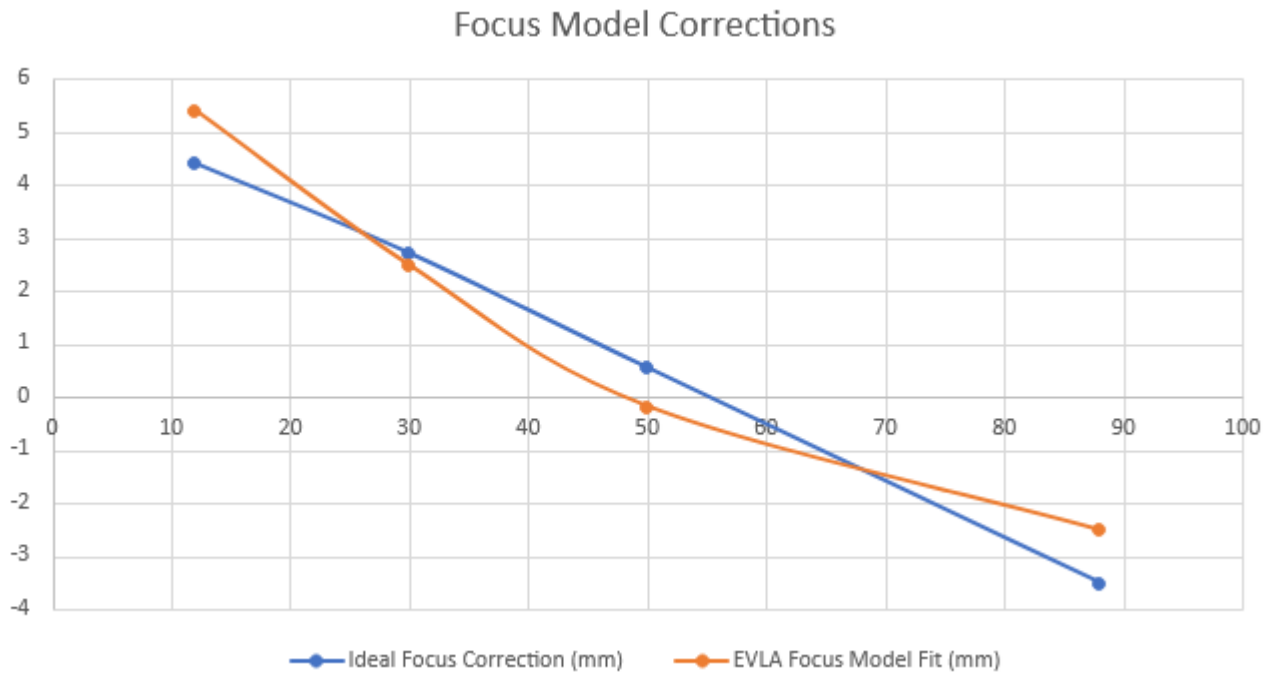

Figure 5: ngVLA prototype antenna focus model Z-axis offset (in mm) as a function of elevation using the current finite element model (calculated by Rob Selina from Robert Lehmensiek's FEA analysis).

9 Subreflector Pointing Error Correction

To compensate for the sag, contraction, and rotation of the prime focus, for many Cassegrain or offset feed telescope systems the position of the subreflector is automatically adjusted using an FEM-based algorithm. An example of the performance and modeling for a standard Cassegrain antenna (the ALMA NA 12 m antennas) is given in Appendix E. For the ngVLA prototype antenna the focus model correction will involve only a Z-axis position offset (made by the frontend positioner) since the subreflector is fixed. The current finite element model for the antennd (from Robert Lehmensiek) indicates that the offsets as a function of position are as shown in Figure 5. A linear fit to the Z-axis offset is $dz = -0.1046E + 5.7627$ mm. Note that this model does not include any temperature-induced deformations. .

10 Conclusion

The antenna pointing system recommendation described in this document provides a framework for assignment of areas of responsibility (contractor and customer) based on experience with characterization, commissioning, and operation of radio telescopes and facilities. Areas of responsibility are assigned based on skill set and ease of maintenance.

Acknowledgements

Thanks to Pat Wallace and Rob Selina for providing valuable input and insight regarding the content of this memo. As he has for over 25 years of interaction with JGM, Pat's insight into the proper implementation of a pointing system has proven yet again to be invaluable. Thank you also to Wes Grammer and Silver Sturgis for pointing out some errors in the prototype and production ngVLA frontend feed positions and coordinate definitions that were corrected in version 1 of this memo.

Change Record

Revision	Date	Author	Section/ Page affected	Remarks
0	2024-10-22	Jeff Mangum	All	Initial version
1	2025-01-16	Jeff Mangum	Section 8, Table 4, Figure 4	Corrected error in upper frequencies and feed offsets listed in Table 4. Updated feed position drawings with latest versions.

References

de Vincente, P., & Barcia, A. 2007, Informe Técnico IT-OAN 2007-26

Emerson, N. J. 2004a, Internal ALMA Report

—. 2004b, Internal ALMA Report

Grammer, W., & Sturgis, S. 2022, (ngVLA) Frontend Conceptual Design Description 020.30.05.00.00-0006-DSN Version C

Greve, A., & Mangum, J. G. 2004, Internal ALMA Report

Lucas, R. Mangum, J. G., & Matthews, H. 2004, Internal ALMA Report

Mangum, J. G. 2001, ALMA Memo 366

—. 2003, Internal Report to Antenna IPT

Mangum, J. G., Baars, J. W. M., Greve, A., et al. 2006, PASP, 118, 1257, doi: 10.1086/508298

Pangole, E. 2003, ALMA-80.05.00.00-009-B-SPE

Rogulenko, E. 2024, (ngVLA) 020.10.40.05.00-0031-ICD version 3.0, 2024-09-20

Selina, R., & Sturgis, S. 2020, (ngVLA) Antenna Coordinate System 020.10.30.00.00-0001-SPE

Stumpff, P. 1972, Kleinheubacher Berichte, 15, 431–437

Sturgis, S. 2025a, MSIP Receiver Enclosure (2025-01-15)-DWG

—. 2025b, ngVLA Receiver Enclosure (2025-01-15)-DWG

Wallace, P. T. 2002, in Society of Photo-Optical Instrumentation Engineers (SPIE) Conference Series, Vol. 4848, Advanced Telescope and Instrumentation Control Software II, ed. H. Lewis, 125–136, doi: 10.1117/12.460914

Wallace, P. T., Mangum, J. G., & Lucas, R. 2004, Internal ALMA Report

White, E., Ghigo, F. D., Prestage, R. M., et al. 2022, A&A, 659, A113, doi: 10.1051/0004-6361/202141936

A `TPOINT` Input Pointing Measurement and Model File Definitions and Formats

The recommended format for ngVLA pointing measurement results is adapted from the format used by ALMA. It corresponds to "format 4" within `TPOINT` and includes only four required values per measurement:. The following is an example pointing measurement file (truncated) from the ALMA prototype antenna evaluation:

```
ALMA Antenna Test Facility: 2003-07-17T03:36:31
: ALTAZ
: ALLSKY
34 4 29.80 !  2003 7 17 23.0 791.3 2000.0 40.216 0.57 0.0065
177.446912923 , 59.3539272854 , 177.405103266 , 59.3646992556
181.521868726 , 60.3416712109 , 181.476930778 , 60.3531384596
201.033701618 , 54.4547067717 , 201.003735802 , 54.4686611257
-70.7474005671 , 62.0219915066 , -70.8158519167 , 62.0339031294
-144.942068618 , 19.9641487927 , -144.937868101 , 19.9796910554
...
END
```

The entries in this file are:

Line 1: Caption record (user defined).

Line 2: An option record (you can have as many of these as you like). `: ALTAZ` defines the antenna mount as Az/El within `TPOINT`.

Line 3: Another option record. `: ALLSKY` disables horizon/zenith/pole checks within `TPOINT`.

Line 4: A run parameters record. The only necessary parameter in this entry is the first three numbers, which represent the antenna latitude (d,m,s). This is followed by a comment entry (identified by a `!`) which listed the date and a measure of the local atmospheric conditions. Note that this information is not used in the pointing model analysis.

Line 5 through n: Observation records which are defined as A_{com}, E_{com}, A_{demand}, E_{demand} (see Section 5).

Last Line: `END` to mark end-of-file.

In the following we list a suggested pointing coefficient file structure. This file is structured such that:

- For maximum flexibility, the pointing coefficient file consists of a list of character strings and numbers. The character strings are the coefficient names (such as "NPAE") and the numbers the coefficients in arcseconds. Comments are designated by a "#" in column 1.
- The model is assumed to be set up dynamically when the system is booted and to contain the full repertoire of terms as defined in the TPOINT program.
- There is no restriction that each antenna has a model of the same form. For the same antenna design most of the terms will be in common, but there is nothing to stop individual antennas from having their own peculiarities.
- The "DATE-OBS" line is user-defined string containing the date/time when the *observations* were made (not when the coefficients were calculated).

- The `T...` line defines what kind of measurements were made, where `T` means that the pointing model corrects the antenna positioning. The numbers which follow the `T` entry are number of measurements used to derive pointing terms, sky RMS (in arcseconds), and two refraction constants in arcseconds (not used for ALMA).
- The pointing coefficients describe the pointing model for a detector located at the boresight of the telescope, even though it is not a requirement for there to actually be a detector at the boresight position. Note that any valid `TPOINT` coefficient can be used in this file.

```
# Pointing Model Coefficients for Antenna n
DATE-OBS 2002-02-20T22:18:39.613
T    246   1.25    0.000   0.0000
IA              xxx.xx
IE              xxx.xx
HECE            xxx.xx
CA              xxx.xx
NPAE            xxx.xx
AN              xxx.xx
AW              xxx.xx
HESE            xxx.xx
HASA            xxx.xx
HACA            xxx.xx
HASA2           xxx.xx
HESA            xxx.xx
HESA3           xxx.xx
```

B Gravitational Deflection of the Vertical

The tilt of the azimuth axis of an antenna is parameterized in a pointing model through the AN and AW pointing terms. These two terms describe the extent to which the azimuth axis is not exactly normal to the geoid. The two main contributions to these two components of the azimuth axis tilt are:

- Any errors made in leveling the azimuth bearing when the antenna was installed on its foundation.
- Local gravity nonuniformities due to nearby geography. This effect is generally referred to as the "gravitational deflection of the vertical".

To provide a working example, Figure 6 shows a sketch of the situation for ALMA. The gravitational influence of the Andes mountains to the east results in a tilt of the local vertical toward the west. This tilt, added to any tilt of the azimuth bearing relative to the local gravity vector, results in a total tilt of the azimuth axis whose western component is AW. Keep in mind that:

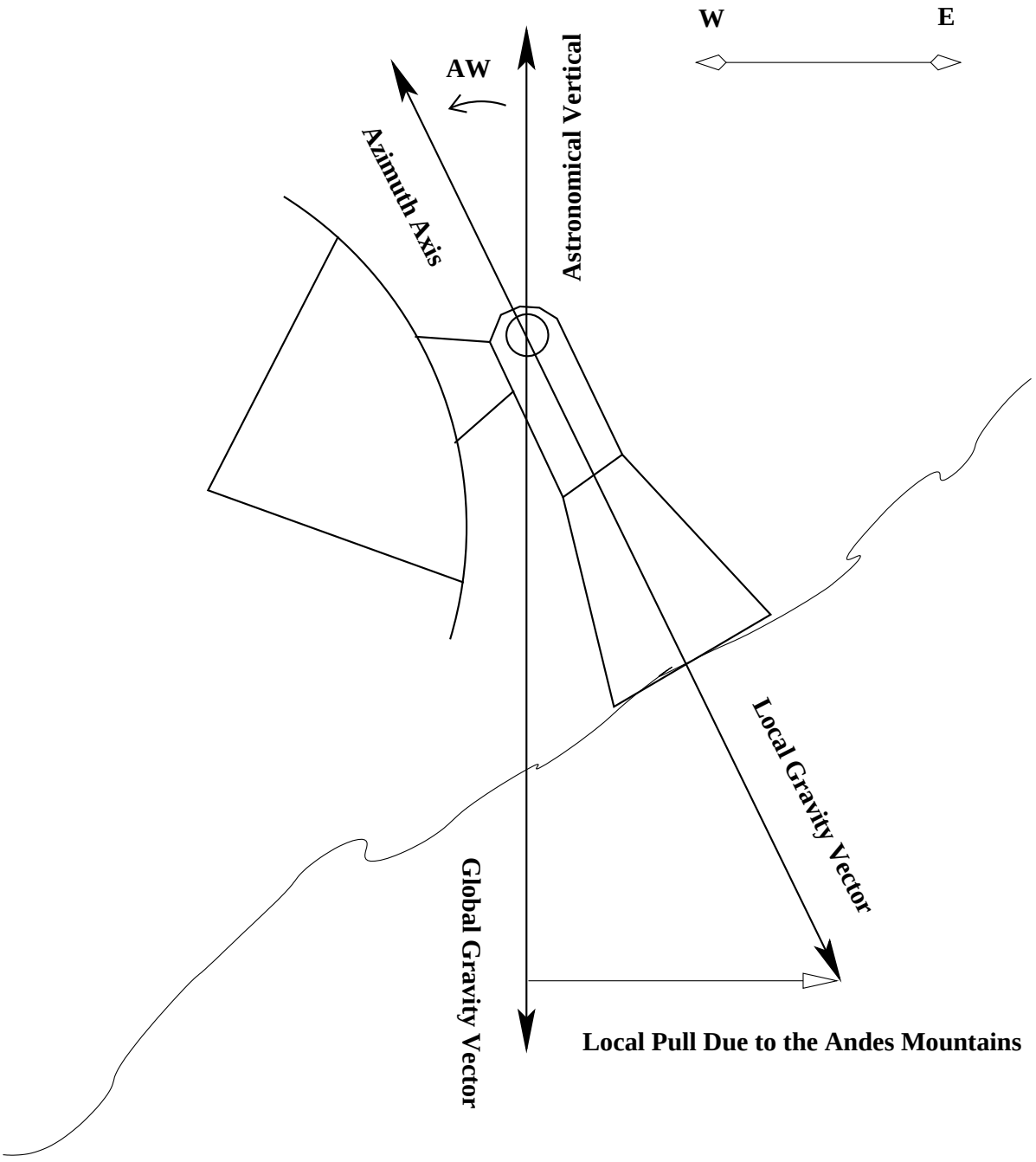

Figure 6: Schematic showing the tilt of the azimuth axis in the ALMA context. This representation assumes that the mount has been accurately leveled. Original design by Nicholas Emerson.

- Tiltmeter measurements of the azimuth structure provide information on the tilt of the azimuth axis relative to local the local gravity vector only.
- AN and AW derived from pointing tests tell us about mount orientation with respect to the normal to the geoid at the specified site coordinates (the "global gravity vector" in Figure 6).
- If tiltmeters designed to report the tilt of the azimuth axis indicate that the azimuth axis is perfectly vertical, AN and AW derived from pointing measurements represent estimates of the gravitational deflection of the vertical.

C The Effect of the Small Angle Approximation

In the following we provide examples of how and when the small-angle approximation fails.

C.1 Rotation Matrices

In the following we will use rotation matrices to define how to transform the (A,E) position toward which an undeformed antenna is pointed to a deformed (A′,E′) position. For clockwise rotations by angles α, β, and δ about the X-, Y-, and Z-axes:

$$p_x = \begin{pmatrix} 1 & 0 & 0 \\ 0 & \cos\alpha & \sin\alpha \\ 0 & -\sin\alpha & \cos\alpha \end{pmatrix} \tag{14}$$

$$p_y = \begin{pmatrix} \cos\beta & 0 & \sin\beta \\ 0 & 1 & 0 \\ -\sin\beta & 0 & \cos\beta \end{pmatrix} \tag{15}$$

$$p_z = \begin{pmatrix} \cos\delta & \sin\delta & 0 \\ -\sin\delta & \cos\delta & 0 \\ 0 & 0 & 1 \end{pmatrix} \tag{16}$$

We will use these rotation matrix equations in the following derivations of the collimation and nonperpendicularity error terms.

C.2 Derivation of the Collimation Error Term CA

The elevation and azimuth collimation offsets of the radiometric beam of an antenna relative to the position of an astronomical source are given by the pointing model terms IE and CA, respectively. The elevation collimation term IE is a simple elevation offset with no other dependencies. For the azimuth collimation offset CA, though, one must employ a rotation matrix analysis to derive its form. As pointed out by de Vincente & Barcia (2007), for a collimation correction CA which moves an antenna from (A,E) to (A′,E′) , where $E' = E + \Delta E$ and $A' = A + \Delta A$, can be described by a combination of three transformations:

1. A rotation about the X-axis by −E, followed by
2. A rotation about the Z-axis by CA, followed by
3. A rotation about the X-axis by +E (thus undoing the first transformation)

which results in the vector p_3:

$$\begin{aligned} p_3 &= \begin{pmatrix} \cos E' \sin A' \\ \cos E' \cos A' \\ \sin E' \end{pmatrix} \\ &= \begin{pmatrix} 1 & 0 & 0 \\ 0 & \cos E & -\sin E \\ 0 & \sin E & \cos E \end{pmatrix} \begin{pmatrix} \cos(CA) & -\sin(CA) & 0 \\ \sin(CA) & \cos(CA) & 0 \\ 0 & 0 & 1 \end{pmatrix} \begin{pmatrix} 1 & 0 & 0 \\ 0 & \cos E & \sin E \\ 0 & -\sin E & \cos E \end{pmatrix} \begin{pmatrix} \cos E \sin A \\ \cos E \cos A \\ \sin E \end{pmatrix} \\ &= \begin{pmatrix} \cos(CA) & -\cos E \sin(CA) & -\sin E \sin(CA) \\ \cos E \sin(CA) & \cos^2 E \cos(CA) + \sin^2 E & \sin E \cos E \left(\cos(CA) - 1\right) \\ \sin E \sin(CA) & \sin E \cos E \left(\cos(CA) - 1\right) & \sin^2 E \cos(CA) + \cos^2 E \end{pmatrix} \begin{pmatrix} \cos E \sin A \\ \cos E \cos A \\ \sin E \end{pmatrix} \end{aligned} \tag{17}$$

To derive the azimuth correction we use $\cos E' \sin A'$ in Equation 17:

$$\cos E' \sin A' = \cos(CA) \cos E \sin A - \cos^2 E \sin(CA) \cos A - \sin^2 E \sin(CA) \tag{18}$$

To derive the elevation correction we use $\sin E'$ in Equation 17:

$$\begin{aligned} \sin E' = {} & \sin E \sin(CA) \cos E \sin A + \sin E \cos^2 E \left(\cos(CA) - 1\right) \cos A \\ & + \left[\sin^2 E \cos(CA) + \cos^2 E\right] \sin E \end{aligned} \tag{19}$$

Inserting A and ΔA in place of A' and E and ΔE in place of E' and solving for ΔE and ΔA:

$$\begin{aligned} \cos(E + \Delta E) \sin(A + \Delta A) = {} & \cos(CA) \cos E \sin A - \cos^2 E \sin(CA) \cos A \\ & - \sin^2 E \sin(CA) \end{aligned} \tag{20}$$

$$\begin{aligned} \sin(E + \Delta E) = {} & \sin E \sin(CA) \cos E \sin A \\ & + \sin E \cos^2 E \left(\cos(CA) - 1\right) \cos A \\ & + \left[\sin^2 E \cos(CA) + \cos^2 E\right] \sin E \end{aligned} \tag{21}$$

One solves for ΔA and ΔE in Equations 20 and 21 and inserts these additional terms in the pointing relations Equations 3 and 4, respectively.

C.3 Approximations

In the following sections we will use the following approximations (where we have used α to represent any of the pointing model coefficients (i.e., CA, NPAE, etc.):

$$\begin{aligned}
\sin(A+\Delta A) &\simeq \sin A\cos(\Delta A)+\cos A\sin(\Delta A)\\
&\simeq \sin A+\cos A\Delta A\\
\cos(E+\Delta E) &\simeq \cos E\cos(\Delta E)-\sin E\sin(\Delta E)\\
&\simeq \cos E-\sin E\Delta E\\
\sin(E+\Delta E) &\simeq \sin E+\cos E\Delta E\\
\cos(\alpha) &\simeq 1-\frac{\alpha^2}{2}\\
\sin(\alpha) &\simeq \alpha-\frac{\alpha^3}{3!}
\end{aligned} \tag{22}$$

C.4 The Effect of the Small Angle Approximation on Azimuth Collimation (CA)

The current ALMA monitor and control software uses the small-angle approximation to effect most of the pointing model corrections. For the collimation term in azimuth (CA), this implies that in practice the correction due to elevation changes is considered to be zero. When this is not the case (i.e.when an OPT system is not correctly aligned to the boresight), the small-angle approximation breaks down and one should use the nonapproximate spherical trigonometric expressions.

The error encountered when using the small-angle approximation when CA becomes large can be estimated using Equation 20 and 21 with $A=0$:

$$\cos(E+\Delta E)\sin(A+\Delta A) = -\sin(CA) \tag{23}$$

$$\begin{aligned}
\sin(E+\Delta E) &= \sin E\left[\cos^2 E\left(\cos(CA)-1\right)+\sin^2 E\cos(CA)+\cos^2 E\right]\\
&= \sin E\cos(CA)
\end{aligned} \tag{24}$$

Substituting the first-order approximations from §C.3 (Equations 22) into Equations 23 and 24:

$$\left(\cos E-\sin E\Delta E\right)\Delta A \simeq -CA+\frac{CA^3}{3!} \tag{25}$$

$$\sin E+\cos E\Delta E \simeq \left(1-\frac{CA^2}{2!}\right)\sin E \tag{26}$$

Solving Equations 25 and 26 for ΔA and ΔE:

$$\Delta A \simeq \frac{CA^3/3!-CA}{\cos E+(CA^2/2)\sin E\tan E} \tag{27}$$

$$\Delta E \simeq -\frac{CA^2}{2}\tan E \tag{28}$$

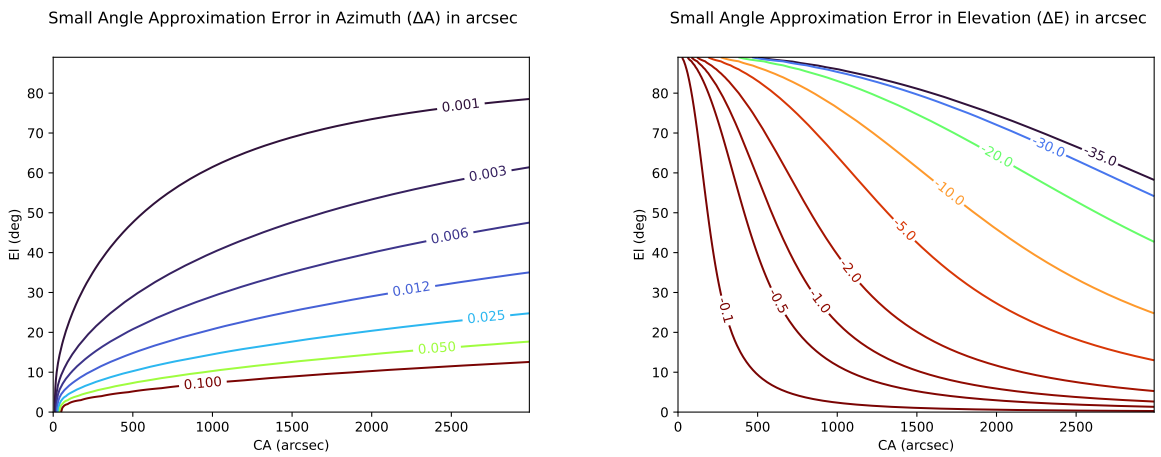

Figure 7: Error made when using the small-angle approximation to calculate the collimation error in azimuth (ΔA; left) and elevation (ΔE; right) as functions of E and CA.

Figure 7 shows Equations 27 and 28 as functions of E and CA. For small CA and ΔE Equations 27 and 28 reduce to the normal collimation correction term in azimuth. The additional term ΔE can be further developed by writing ΔE and CA in terms of arcsec:

$$\begin{aligned}\Delta E(arcsec) &\simeq -\frac{CA^2(arcsec)}{2}\left(\frac{\pi}{180\times 3600}\right)\tan E \\ &\simeq -\left(\frac{CA(arcsec)}{642.3}\right)^2 \tan E \end{aligned} \tag{29}$$

Since it is the "differential" correction that is important (for offset pointing measurements, for example), what one wants to know is what the derivative of Equation 29 is with respect to changes in elevation. Calculating this derivative we get:

$$\begin{aligned}\frac{d(\Delta E)}{dE} &\simeq -\left(\frac{CA}{642.3}\right)^2 \sec^2 E \\ d(\Delta E) &\simeq -\left(\frac{CA}{642.3}\right)^2 \sec^2 E \left(\frac{\pi}{180}\right) dE \\ &\simeq -\left(\frac{CA}{4861.8}\right)^2 \sec^2 E dE \end{aligned} \tag{30}$$

where dE is in degrees, CA in arcsec, and $d(\Delta E)$ in arcsec. Figure 8 shows a calculation of Equation 30 for dE of 2 degrees. A few representative values for $dE = 2$ degrees on an antenna with $CA = -1150$ arcsec (which was a measured collimation pointing term for the optical pointing telescope on one of the Vertex antennas) leads to ΔE values as follows:

- $\Delta E = -0.22$ arcsec for $E = 45$ degrees

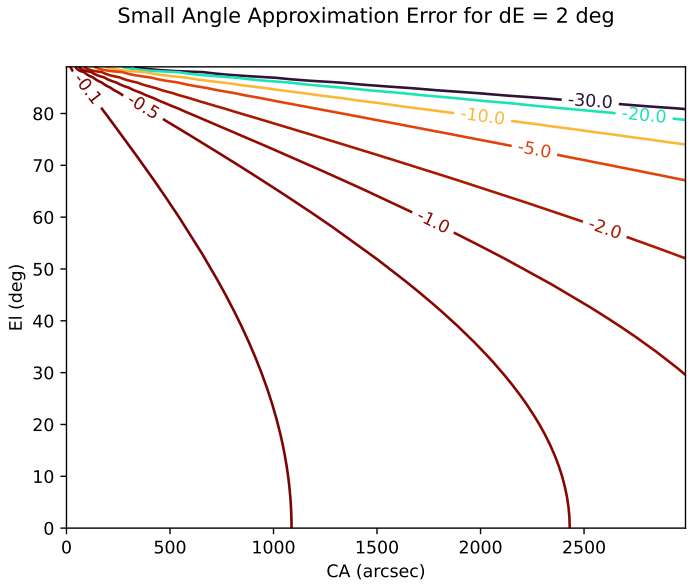

Figure 8: Error made when using the small-angle approximation to calculate the collimation error in azimuth for a source separation of 2 degrees.

- $\Delta E = -0.34$ arcsec for $E = 55$ degrees
- $\Delta E = -0.63$ arcsec for $E = 65$ degrees
- $\Delta E = -1.67$ arcsec for $E = 75$ degrees

Clearly at moderate to high elevation the error made in using the small-angle approximation becomes significant.

C.5 Derivation of the Non-Perpendicularity Term NPAE and the Effect of the Small Angle Approximation

Similar to how we derived the collimation error term in Section C.2, the non-perpendicularity error term is derived by performing a counter-clockwise rotation by an angle NPAE about the Y-axis. Using Equation 15:

$$\begin{aligned} p_1 &= \begin{pmatrix} \cos E' \sin A' \\ \cos E' \cos A' \\ \sin E' \end{pmatrix} \\ &= \begin{pmatrix} \cos(NPAE) & 0 & -\sin(NPAE) \\ 0 & 1 & 0 \\ \sin(NPAE) & 0 & \cos(NPAE) \end{pmatrix} \begin{pmatrix} \cos E \sin A \\ \cos E \cos A \\ \sin E \end{pmatrix} \end{aligned} \tag{31}$$

Noting that $E' = E + \Delta E$ and $A' = A + \Delta A$, the error in A and E are given by:

$$\cos(E + \Delta E) \sin(A + \Delta A) = \cos(NPAE) \cos E \sin A - \sin(NPAE) \sin E \tag{32}$$

$$\sin(E + \Delta E) = \sin(NPAE) \cos E \sin A + \cos(NPAE) \sin E \tag{33}$$

For A = 0 and using some of the approximations listed in Equation 22, Equations 32 and 33 become:

$$(\cos E - \sin E \Delta E)\, \Delta A \simeq \left(-NPAE + \frac{NPAE^3}{3!}\right) \sin E \tag{34}$$

$$\sin E + \cos E \Delta E \simeq \left(1 - \frac{NPAE^2}{2!}\right) \sin E \tag{35}$$

Solving for ΔA and ΔE in Equations 34 and 35, respectively:

$$\Delta A \simeq \frac{(NPAE^3/3! - NPAE) \sin E}{\cos E + (NPAE^2/2) \tan E} \tag{36}$$

$$\Delta E \simeq -\left(\frac{NPAE^2}{2}\right) \sec E \tag{37}$$

Note that for small NPAE that the equation for ΔA (Equation 36) reduces to the usual non-perpendicularity term in our pointing model. Figure 9 shows Equations 36 and 37 as functions of E and NPAE.

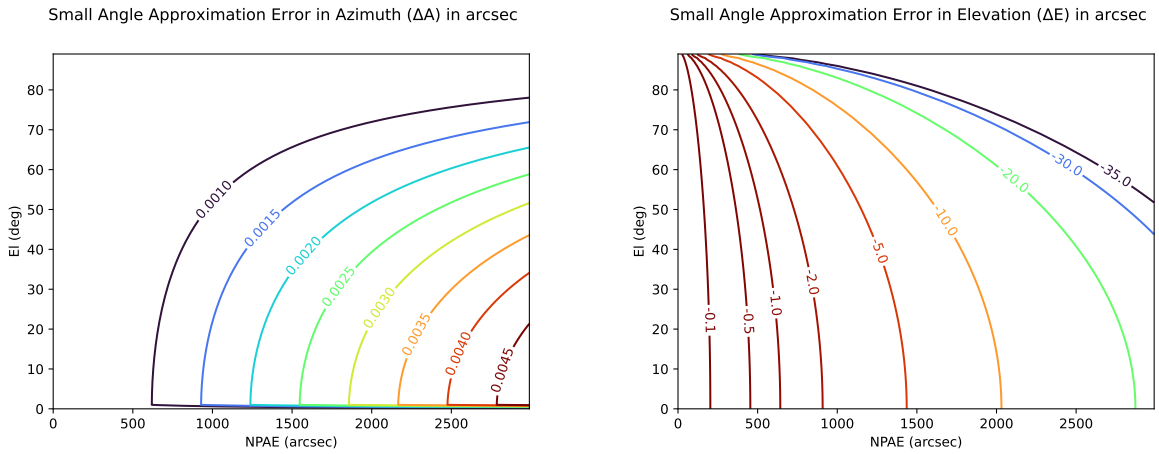

Figure 9: Error made when using the small-angle approximation to calculate the collimation error in azimuth (ΔA; left) and elevation (ΔE; right) as functions of E and NPAE.

D Tiltmeter Calibration

Tiltmeter calibration can be done in one of two ways:

D.1 Slow Ride

1. Acquire measurements of the tiltmeter output taken in one of two ways:

(a) During an all-sky pointing run or

(b) During a slow rotation test, where the antenna was pointed to zenith and slowly rotated 360 degrees first clockwise then counter-clockwise in azimuth,

2. Perform a least-squares fit of each tiltmeter axis measurement to a sinusoidal model:

$$T1_x = ax * \sin(A + cx) + dx \quad (38)$$
$$T1_y = ay * \sin(A + cy) + dy \quad (39)$$

where:

- $T1_x$ is the tiltmeter 1 X axis measurement (from ACU report).
- $T1_y$ is the tiltmeter 1 Y axis measurement (from ACU report).
- ax, ay, bx, and by are the differential tiltmeter measurements (relative to the sinusoidal model).
- dx and dy are the tiltmeter installation alignment offsets along the X and Y axes, respectively. These correspond to rotation around the IE (for dx) and NPAE (for dy) axes. Both can vary slightly, presumably due to thermal gradients in the yoke.

This gives one the scale (ax,ay), phase (cx,cy), and offset (dx,dy) parameters which can then be used in a least-squares fit.

3. Noting that:

$$T1_x - dx = -AN_0 \cos(A) + AW_0 \sin(A) \quad (40)$$
$$T1_y - dy = -AN_0 \sin(A) - AW_0 \cos(A) \quad (41)$$

do a least-squares fit to the sum of these two equations to derive AN0 and AW0:

$$T1_x - dx + T1_y - dy = -AN_0 (\cos(A) + \sin(A)) + AW_0 (\sin(A) - \cos(A)) \quad (42)$$

An example of fits to four such dedicated azimuth rotation test measurements, measured at 10:00, 14:00, 18:00, and 22:00 UT on 2010-10-16 with DV10, are as follows:

```
[ax,cx,dx] =  [-17.33773662  -1.17824341   1.77411825]
(units are arcsec, radians, arcsec)
[ay,cy,dy] =  [ 16.19570775   0.36913804  -0.16827352]
(units are arcsec, radians, arcsec)
[AN0,AW0] =  [-15.16738523  -6.69516468]  (units are arcsec, arcsec)
SA2 =  -0.107628808002  arcsec
SA3 =  -0.203185092595  arcsec
phi2 =  -5.39700759443  deg
phi3 =  44.8901004946  deg
offset =  8.43305189254  arcsec
```

```
[ax,cx,dx] =  [-16.20987898  -1.31667739   2.08921298]
(units are arcsec, radians, arcsec)
[ay,cy,dy] =  [ 15.17594569   0.23453498   1.73126987]
(units are arcsec, radians, arcsec)
[AN0,AW0] =  [-14.95073548  -4.26531491]  (units are arcsec, arcsec)
SA2 =  -0.119268904962  arcsec
SA3 =  -0.14033049032  arcsec
phi2 =  -2.88163744871  deg
phi3 =  27.362196717  deg
offset =  10.2047262563  arcsec

[ax,cx,dx] =  [ -16.6913208  -1.29153294e+00   1.20923671e-02]
(units are arcsec, radians, arcsec)
[ay,cy,dy] =  [ 15.6074545    0.25458207   0.51958835]
(units are arcsec, radians, arcsec)
[AN0,AW0] =  [-15.23937805  -4.73589655]  (units are arcsec, arcsec)
SA2 =  -0.12101499162  arcsec
SA3 =  -0.0962365999835  arcsec
phi2 =  -1.25470515551  deg
phi3 =  16.1934346415  deg
offset =  6.36057539222  arcsec

[ax,cx,dx] =  [-19.63631011  -1.21689739  -1.08563871]
(units are arcsec, radians, arcsec)
[ay,cy,dy] =  [ 18.40696169   0.32845335  -1.48090653]
(units are arcsec, radians, arcsec)
[AN0,AW0] =  [-17.48749148  -6.86963734]  (units are arcsec, arcsec)
SA2 =  -0.117467834563  arcsec
SA3 =  -0.147038272493  arcsec
phi2 =  -11.0735981655  deg
phi3 =  20.9741151557  deg
offset =  7.24358941887  arcsec
```

Note that the fit to these measurements includes a fit to the linear sensor correction curve. Figures 10, 11, 12 and 13 show plots of the fit and residuals to the four example datasets described above. For the results from the four runs shown above we can derive AN0 $= -15.71 \pm 1.19$ arcsec and AW0 $= -5.64 \pm 1.33$ arcsec.

D.2 Cardinal Rule

1. Acquire measurements of the tiltmeter output taken when the antenna is pointed to elevation 45 degrees and each of the four "cardinal" azimuth positions: 0, 90, 180, and 270 degrees.

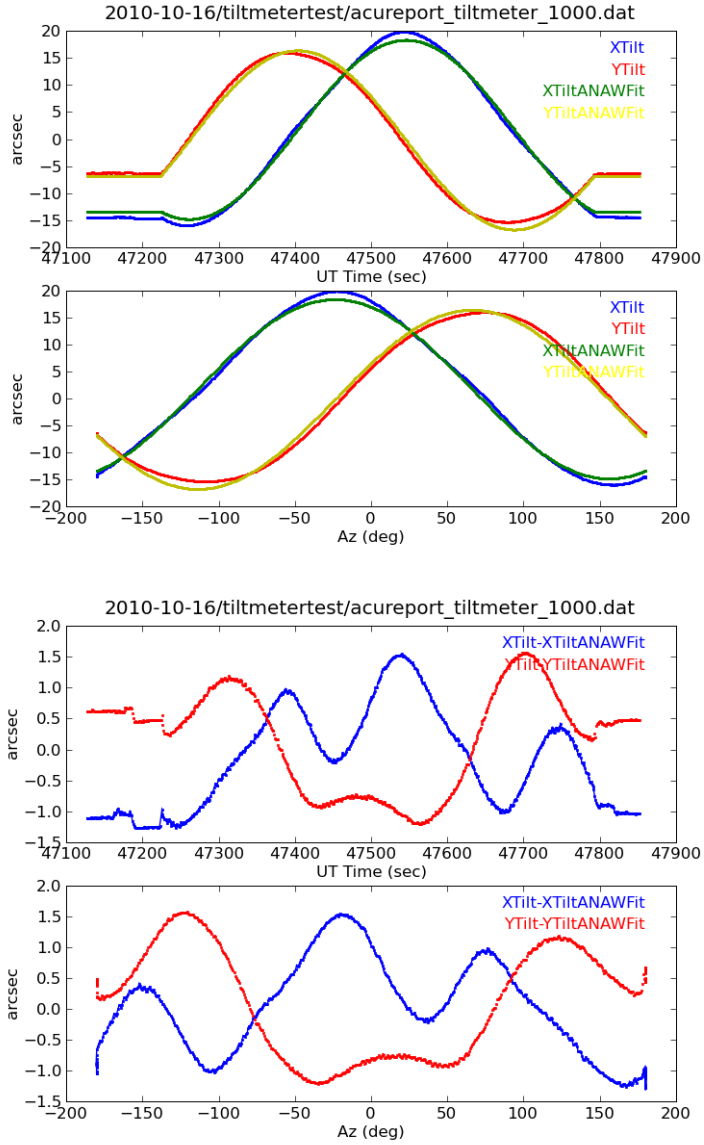

Figure 10: For DV10 tiltmeter calibration measurements run 2010-10-16 10:00 UT. Top: A comparison of the raw tiltmeter measurements (blue and red curves) and the fits to those measurements (green and yellow curves) as functions of both time (top panel) and azimuth (bottom panel). Bottom: Fit residuals from the top plot. The tiltmeter temperature during this run was 15.90 C throughout.

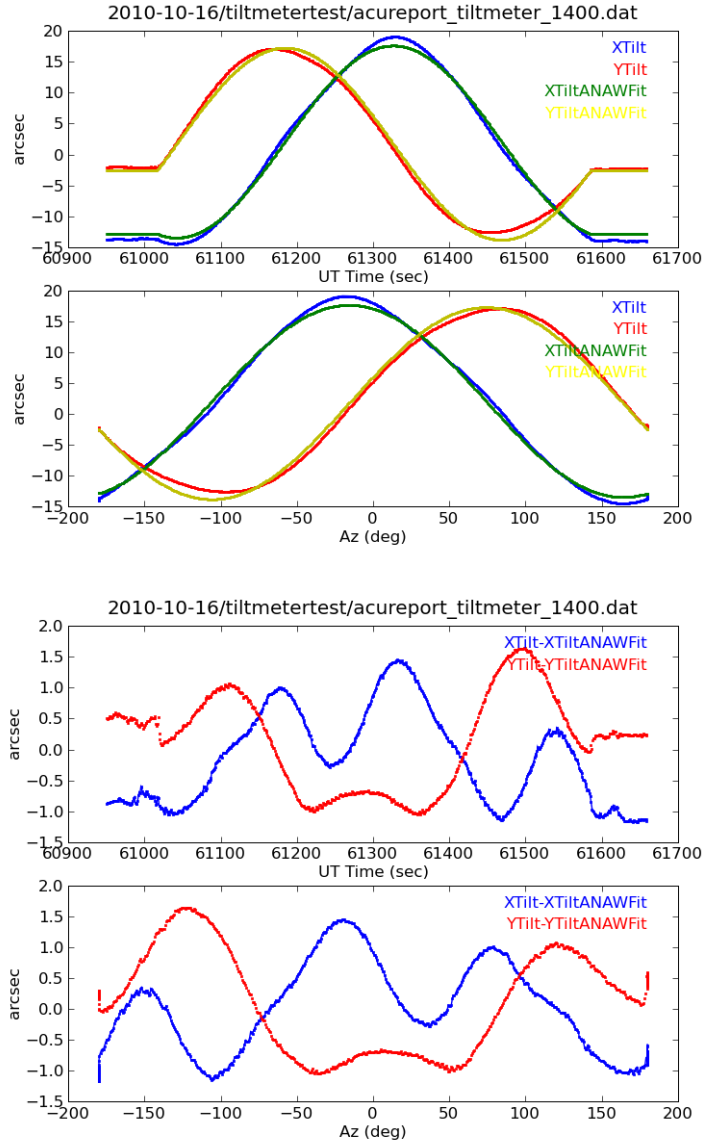

Figure 11: For DV10 tiltmeter calibration measurements run 2010-10-16 14:00 UT. Top: A comparison of the raw tiltmeter measurements (blue and red curves) and the fits to those measurements (green and yellow curves) as functions of both time (top panel) and azimuth (bottom panel). Bottom: Fit residuals from the top plot. The tiltmeter temperature during this run was 16.00 C throughout.

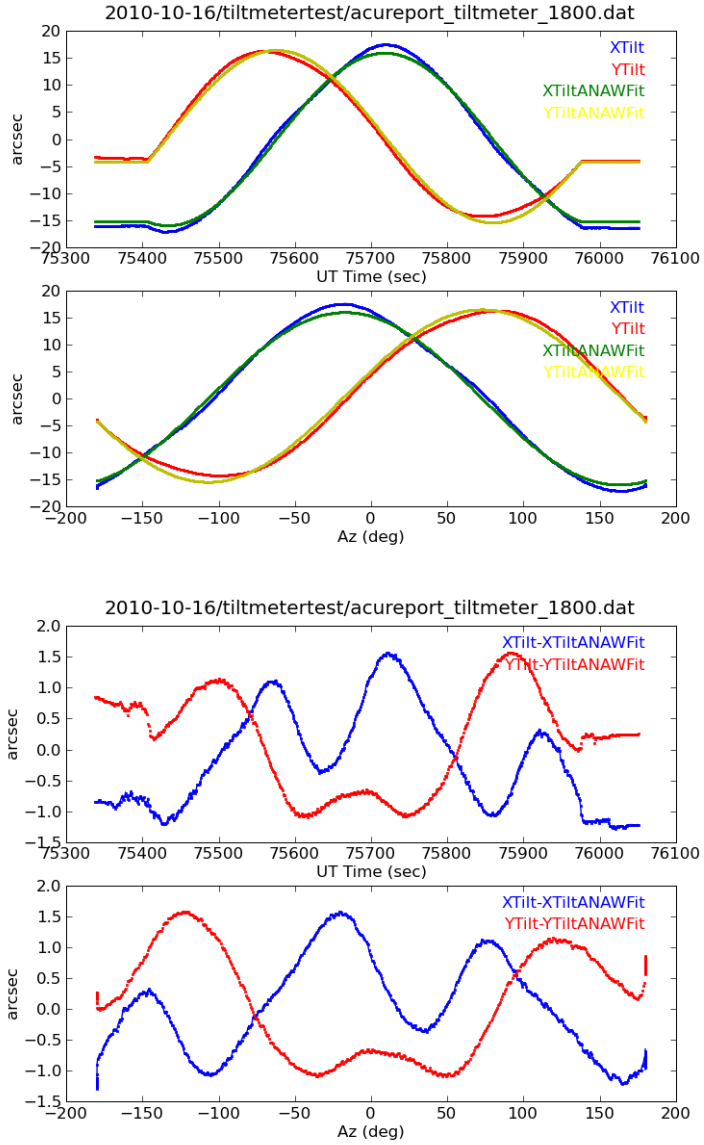

Figure 12: For DV10 tiltmeter calibration measurements run 2010-10-16 18:00 UT. Top: A comparison of the raw tiltmeter measurements (blue and red curves) and the fits to those measurements (green and yellow curves) as functions of both time (top panel) and azimuth (bottom panel). Bottom: Fit residuals from the top plot. The tiltmeter temperature during this run was 17.70 to 17.80 C throughout.

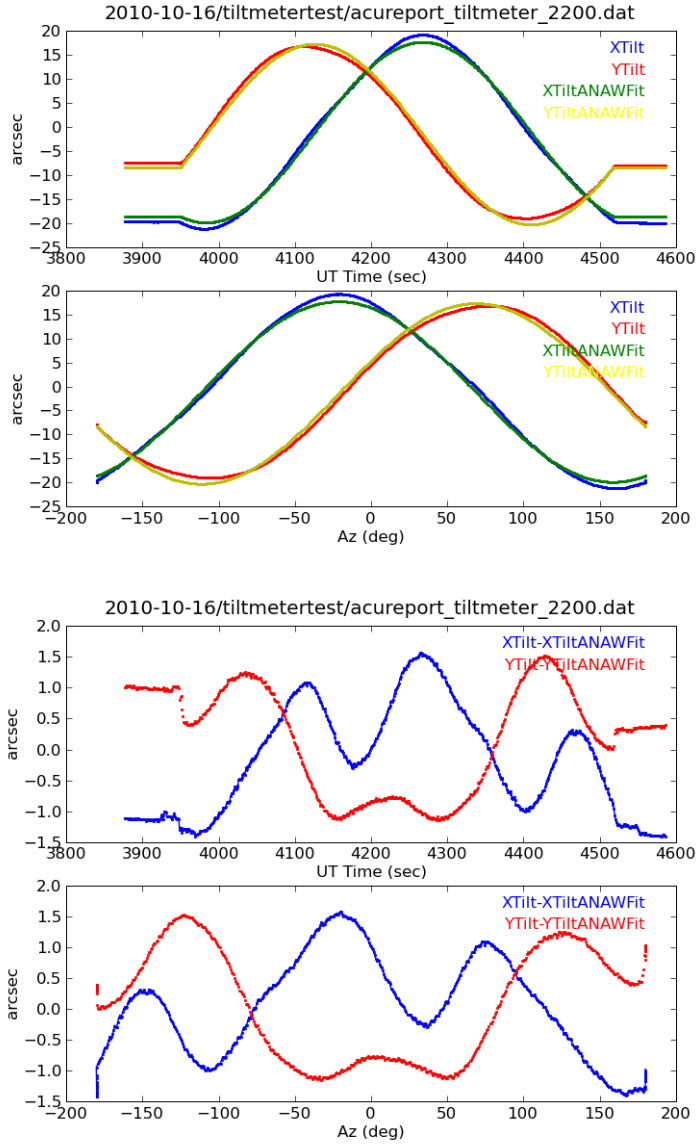

Figure 13: For DV10 tiltmeter calibration measurements run 2010-10-16 22:00 UT. Top: A comparison of the raw tiltmeter measurements (blue and red curves) and the fits to those measurements (green and yellow curves) as functions of both time (top panel) and azimuth (bottom panel). Bottom: Fit residuals from the top plot. The tiltmeter temperature during this run was 18.60 C throughout.

2. Using Equations 41, we can insert values for A=0, 90, 180, and 270 to get the following set of eight equations:

$$T1_x^0 - dx = -AN_0 \tag{43}$$
$$T1_y^0 - dy = -AW_0 \tag{44}$$
$$T1_x^{90} - dx = +AW_0 \tag{45}$$
$$T1_y^{90} - dy = -AN_0 \tag{46}$$
$$T1_x^{180} - dx = +AW_0 \tag{47}$$
$$T1_y^{180} - dy = +AN_0 \tag{48}$$
$$T1_x^{270} - dx = -AW_0 \tag{49}$$
$$T1_y^{270} - dy = +AN_0 \tag{50}$$

...which allows us to solve for AN_0 by subtracting the first and fifth or fourth and eighth equations:

$$AN_0 = \frac{T1_x^{180} - T1_x^0}{2} \tag{51}$$
$$= \frac{T1_y^{270} - T1_y^{90}}{2} \tag{52}$$

...while AW_0 is derived by subtracting the second and sixth or third and seventh equations:

$$AW_0 = \frac{T1_y^{180} - T1_y^0}{2} \tag{53}$$
$$= \frac{T1_x^{270} - T1_x^{90}}{2} \tag{54}$$

Using Equations 50 we can also derive expressions for dx and dy. Solve for dx by adding the first and fifth or fourth and eighth equations:

$$dx = \frac{T1_x^{180} + T1_x^0}{2} \tag{55}$$
$$= \frac{T1_y^{270} + T1_y^{90}}{2} \tag{56}$$

...and for dy by adding the second and sixth or third and seventh equations:

$$dy = \frac{T1_y^{180} + T1_y^0}{2} \tag{57}$$
$$= \frac{T1_x^{270} + T1_x^{90}}{2} \tag{58}$$

Equations 52, 54, 56, and 58 are the relations spat out by the tiltmeter calibration script *dvTiltmeterCal.py*.

For the Slow Ride tiltmeter calibration measurements described in §D.1 we have made *dvTiltmeterCal.py* measurements proceeding each of the four Slow Ride measurements described. The results from the fits to these contemporaneous Cardinal Rule measurements are as follows:

```
ANo =                  -15.675  arcsec
AWo =                  -5.4975  arcsec
Tiltmeter X offset =  1.895  arcsec
Tiltmeter Y offset =  0.0025  arcsec

ANo =                  -15.005  arcsec
AWo =                  -2.865  arcsec
Tiltmeter X offset =  2.105  arcsec
Tiltmeter Y offset =  1.935  arcsec

ANo =                  -15.3575  arcsec
AWo =                  -3.525  arcsec
Tiltmeter X offset =  0.1125  arcsec
Tiltmeter Y offset =  1.03  arcsec

ANo =                  -17.815  arcsec
AWo =                  -5.245  arcsec
Tiltmeter X offset =  -1.04  arcsec
Tiltmeter Y offset =  -1.215  arcsec
```

For the results from the four Cardinal Rule runs shown above we can derive AN0 $= -15.96 \pm 1.26$ arcsec and AW0 $= -4.28 \pm 1.29$ arcsec. These derived AN0 and AW0 values are in agreement, within uncertainties, of those derived from the Slow Ride measurements taken contemporaneously.

E ALMA Subreflector Pointing Error Correction

To compensate for the sag, contraction, and rotation of the prime focus, for many Cassegrain or offset feed telescope systems the position of the subreflector is automatically adjusted using an FEM-based algorithm. As an example, Equations 59 through 63 list the gravity-induced deformations which describe the ALMA North American antennas. Table 5 lists the coefficients used in Equations 59 through 63. Figure 14 shows a plot of these equations. A similar model which describes temperature-induced deformations of the secondary reflector interface is also often provided by antenna contractors. A demonstration of the radiometric verification of secondary reflector deformation models for the ALMA North American prototype antennas can be found in Lucas & Matthews (2004) and Mangum et al. (2006).

$$\text{X Tilt (arcsec)} = a_{tx} + b_{tx} * \cos(c_{tx} * EL + d_{tx}) \quad (59)$$

$$\text{Y Tilt (arcsec)} = a_{ty} + b_{ty} * \cos(c_{ty} * EL + d_{ty}) \quad (60)$$

$$\text{X (mm)} = a_{px} + b_{px} * \cos(c_{px} * EL + d_{px}) \quad (61)$$

$$\text{Y (mm)} = a_{py} + b_{py} * \cos(c_{py} * EL + d_{py}) \quad (62)$$

$$\text{Z (mm)} = a_{pz} + b_{pz} * \cos(c_{pz} * EL + d_{pz}) \quad (63)$$

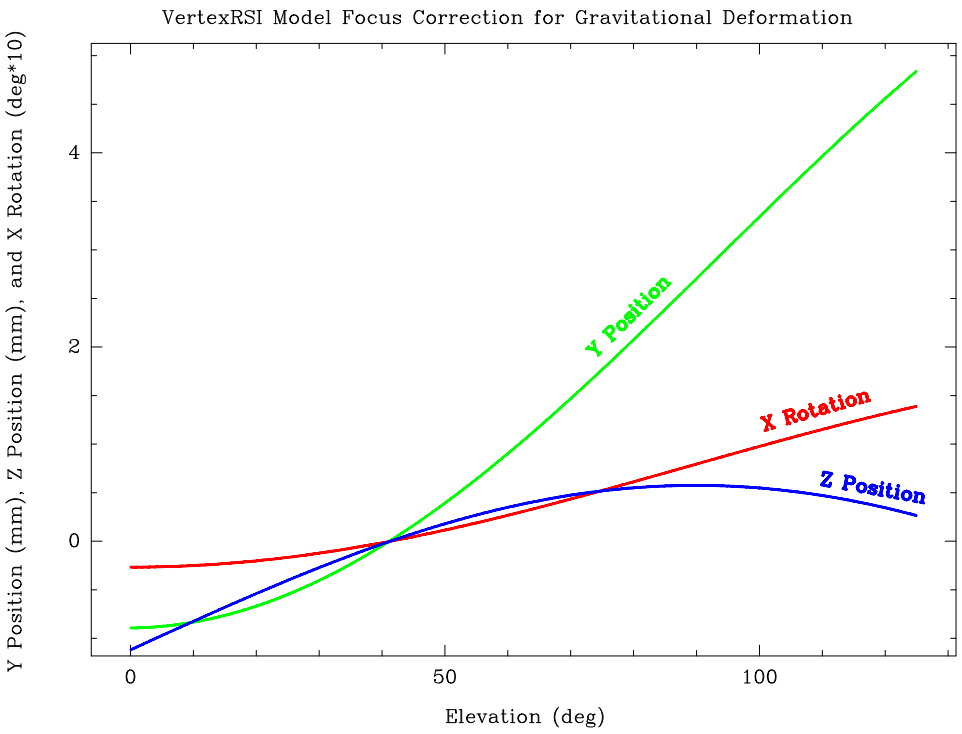

Figure 14: Vertex model subreflector correction (X-tilt, Y, and Z components only, derived from the Vertex prototype).

Table 5: ALMA NA Subreflector Pointing Error Correction Term Coefficients

Term	Value
a_{tx}	274.7680 arcsec
b_{tx}	370.9860 arcsec
c_{tx}	-1.0182
d_{tx}	-3.1435 radians
a_{py}	2.9180 mm
b_{py}	-3.8120 mm
c_{py}	0.9570
d_{py}	0.0116 radians
a_{pz}	-1.1030 mm
b_{pz}	1.6780 mm
c_{pz}	1.0078
d_{pz}	-1.5802 radians